ARTICLE IN PRESS

Journal of the European Ceramic Society xxx (xxxx) xxx–xxx

Contents lists available at ScienceDirect

Journal of the European Ceramic Society

journal homepage: www.elsevier.com/locate/jeurceramsoc

Original Article

Sintering behaviour and microwave dielectric properties of $BaAl_{2-2x}(ZnSi)_xSi_2O_8$ ceramics

Xiao-Qiang Song[a,b], Wen-Zhong Lu[a,b], Xiao-Chuan Wang[a,b], Xiao-Hong Wang[a,b], Gui-Fen Fan[a,b], Raz Muhammad[c], Wen Lei[a,b,*]

[a] School of Optical and Electronic Information, Huazhong University of Science and Technology, Wuhan 430074, PR China
[b] Key Lab of Functional Materials for Electronic Information (B), Ministry of Education, Wuhan 430074, PR China
[c] Department of Physics, Abdul Wali Khan University, Mardan, KP, Pakistan

ARTICLE INFO

Keywords:
$BaAl_2Si_2O_8$
Sintering behaviour
Microwave dielectric properties

ABSTRACT

$BaAl_{2-2x}(ZnSi)_xSi_2O_8$ (x = 0.2–1.0) ceramics were prepared using the conventional solid-state reaction method. The sintering behaviour, phase composition and microwave dielectric properties of the prepared compositions were then investigated. All compositions showed a single phase except for $x = 0.8$. By substituting $(Zn_{0.5}Si_{0.5})^{3+}$ for Al^{3+} ions, the optimal sintering temperatures of the compositions decreased from 1475 °C ($x = 0$) to 1000 °C ($x = 0.8$), which then slightly increased to 1100 °C ($x = 1.0$). Moreover, the phase stability of $BaAl_2Si_2O_8$ was improved. A novel $BaZnSi_3O_8$ microwave dielectric ceramic was obtained at the sintering temperature of 1100 °C. This ceramic possesses good microwave dielectric properties with $\varepsilon_r = 6.60$, $Q \times f = 52401$ GHz (at 15.4 GHz) and $\tau_f = -24.5$ ppm/°C.

1. Introduction

Low-permittivity ($\varepsilon_r < 15$) microwave dielectric ceramics are key materials for microwave wireless communication in the form of high-frequency substrates, dielectric antennae, high-accuracy capacitors and millimeter-wave components such as resonators and filters [1]. As the operating frequency ranges of microwave wireless communication expand, the high performance of microwave dielectric ceramics with low permittivity has attracted much attention.

Usually, silicate has low relative permittivity due to the Si—O bond, which comprises 45% ionic bond and 55% covalent bond strength [2]. Recently, many silicates, such as willemite (Zn_2SiO_4), forsterite (Mg_2SiO_4) and diopside ($CaMgSi_2O_6$) [3–5], have been explored as potential candidates for millimeter-wave devices given their low permittivity and high quality factor.

Celsian ($BaAl_2Si_2O_8$), a natural plagioclase-feldspar mineral, is used as environmental barrier coating, $BaAl_2Si_2O_8$: Eu^{2+} phosphor and matrix material in fibre-reinforced composites [6–8]. At present, the thermal, optical and mechanical properties of celsian ceramics have received considerable research attention, whereas their dielectric properties have been investigated in only a few studies. In 2000, McCauley reported the dielectric properties of $Ba_{1-x}Sr_xAl_2Si_2O_8$ solid solutions [9]. From 2005 to 2009, Krzmanc et al. [10–14] systematically investigated the crystal structure and microwave dielectric properties of plagioclase-feldspar-based ceramics and found that $BaAl_2Si_2O_8$ ceramics exhibit high $Q \times f$ value when sintered at 1500 °C for 40 h. Lei et al. [15] prepared near-zero shrinkage $BaAl_2Si_2O_8$ microwave dielectric ceramics at a sintering temperature of 1475 °C using ethanol as a dispersant. Although $BaAl_2Si_2O_8$ and other plagioclase-feldspar-based ceramics possess good microwave dielectric properties, their commercial application is hindered by some problems. For example, the sintering temperature of $Ba_{1-x}M_xAl_2Si_2O_8$ (M = Ca, Sr; $0 \le x \le 1.0$) solid solutions is approximately 1500 °C, which strictly calls for high energy consumption and the requirement of an equipment. Although $K_xBa_{1-x}Ga_{2-x}Ge_{2+x}O_8$ ($0 \le x \le 1.0$) solid solutions have good microwave dielectric properties and low sintering temperature, their raw materials, such as Ga_2O_3 and GeO_2, are expensive. $Na_xCa_{1-x}Al_{2-x}Si_{2+x}O_8$ ($0 \le x \le 1.0$) solid solutions with low sintering temperature have a maximum quality factor value of only 17600 GHz.

Hence, a feasible solution to these problems is to decrease the sintering temperature of $BaAl_2Si_2O_8$ ceramics and keep the high $Q \times f$ value. Similar to $BaAl_2Si_2O_8$, Al-containing ceramics and aluminates, such as $Sr_2Al_2SiO_7$, MAl_2O_4 (M = Mg, Zn), and $Y_3Al_5O_{12}$ [16–19], have ultra-high sintering temperatures owing to their strong Al—O bonds and high lattice energy. Aluminum content has an important effect on sintering temperature. In addition to sintering temperature, the phase transition of $BaAl_2Si_2O_8$ is another notable problem for us. $BaAl_2Si_2O_8$ has three different phases—hexagonal, monoclinic and orthorhombic.

* Corresponding author at: School of Optical and Electronic Information, Huazhong University of Science and Technology, Wuhan 430074, PR China.
E-mail address: wenlei@mail.hust.edu.cn (W. Lei).

http://dx.doi.org/10.1016/j.jeurceramsoc.2017.10.053
Received 7 May 2017; Received in revised form 17 October 2017; Accepted 26 October 2017
0955-2219/

Please cite this article as: Song, X.-Q., Journal of the European Ceramic Society (2017), http://dx.doi.org/10.1016/j.jeurceramsoc.2017.10.053

Hexagonal celsian can coexist with monoclinic celsian at temperatures below 1590 °C. A reversible phase transition will occur between the hexagonal and orthorhombic phases at about 300 °C; this phase transition is accompanied by a violent volume change [20]. Therefore, the phase transition of celsian will cause microcracks and degrade its microwave dielectric properties.

Reducing Al proportion in the compound is a proper method of decreasing the sintering temperature and adjusting the phase transition. In 1979, Sclar demonstrated the substitution mechanism, by which, $(Fe_{0.5}Si_{0.5})^{3+}$ ions replaced Al^{3+} ions in $CaAl_2Si_2O_8$ [21]. The manufacturing temperature of $CaAl_{2-2x}(FeSi)_xSi_2O_8$ ($0 \le x \le 1.0$) ceramics ranges from 1050 °C to 1200 °C. This work provided a new approach to decrease the sintering temperature of Al-containing ceramics and form a new $CaFeSi_3O_8$ phase. Liu et al. [22,23] substituted Al^{3+} in $SrLaAl_{1-x}(Zn_{0.5}Ti_{0.5})_xO_4$ ceramics with $(Zn_{0.5}Ti_{0.5})^{3+}$ and obtained a new $SrLa(Zn_{0.5}Ti_{0.5})O_4$ phase. With the exception of the end member $CaFeSi_3O_8$ in $CaAl_{2-2x}(FeSi)_xSi_2O_8$ ($0 \le x \le 1.0$) ceramics, the existence of $CaZnSi_3O_8$, $BaZnSi_3O_8$ and $CaMgSi_3O_8$ [24–27] have been confirmed by previous studies. $AMSi_3O_8$ (A = Ca, Ba; M = Mg, Zn, Fe) is a new type of plagioclase-feldspar material, which has a similar structure to $MAl_2Si_2O_8$ (M = Ca, Sr, Ba) and medium sintering temperature, thus provides the feasible option of lowering the sintering temperature and stabilizes the phase composition of $BaAl_2Si_2O_8$ ceramics by forming a solid solution between $BaAl_2Si_2O_8$ and $BaZnSi_3O_8$.

Therefore, $(Zn_{0.5}Si_{0.5})^{3+}$ ions were used to substitute the Al^{3+} ions, and $BaAl_{2-2x}(ZnSi)_xSi_2O_8$ (x = 0.2–1.0) solid solutions were prepared through the conventional solid-state reaction method. The sintering behaviour, phase composition, and microwave dielectric properties of $BaAl_{2-2x}(ZnSi)_xSi_2O_8$ (x = 0.2–1.0) ceramics were investigated.

2. Experimental procedure

The $BaAl_{2-2x}(ZnSi)_xSi_2O_8$ (x = 0.2–1.0) ceramics were prepared by conventional solid-state method using reagent grade $BaCO_3$ (99.8%), Al_2O_3 (99.5%), ZnO (99.5%), and SiO_2 (99.5%) powders as raw materials. According to the stoichiometry, the raw materials were weighed to ball milled in a polyethylene jar for 12 h using ZrO_2 balls with deionized water. After drying at 85 °C, the mixtures were calcined in the temperature range of 950 °C–1100 °C for 3 h with a heat rate of 5 °C/min. And then the powders were uniaxially pressed into samples with dimensions of 12 mm in diameter, and 6 mm in height under a pressure of 150 MPa. The samples were sintered in the temperature range of 980 °C–1250 °C for 3 h at a heating rate of 5 °C/min in air, they were cooled at a rate of 1 °C/min down to 1000 °C and then at a rate of 2 °C/min down to 800 °C, finally naturally cooled in the furnace. The XRD data were obtained using X-ray diffraction (XRD, XRD–7000, Shimadzu, Kyoto, Japan) using CuKα radiation. The microstructure was observed by scanning electron microscope (SEM, Sirion 200, Netherlands) and grain size distributions was obtained using Image J. The ε_r and the unloaded $Q \times f$ value were measured at about 15 GHz in the TE_{011} mode by Hakki and Coleman method [28] using a network analyzer (Agilent E8362B, Agilent Technologies, USA) and parallel silver boards. The τ_f value in the temperature range of 30–80 °C was calculated by Formula (1):

$$\tau_f = \frac{1}{f(T_0)} \frac{[f(T_1) - f(T_0)]}{T_1 - T_0} \tag{1}$$

where $f(T_1)$ and $f(T_0)$ represent the resonant frequency at T_1 (80 °C) and T_0 (30 °C), respectively.

3. Results and discussion

The XRD patterns of the $BaAl_{2-2x}(ZnSi)_xSi_2O_8$ (x = 0.2–1.0) ceramics sintered at different densification temperatures are shown in Fig. 1. The diffraction peaks that corresponded to $BaAl_{2-2x}(ZnSi)_xSi_2O_8$ (x = 0.2–0.6) were indexed to monoclinic $BaAl_2Si_2O_8$ (PDF#38-1450), and the XRD peaks of $BaAl_{2-2x}(ZnSi)_xSi_2O_8$ (x = 1.0) agreed well with that of $BaZnSi_3O_8$ (PDF#23-0481), which exhibited a lower symmetry than $BaAl_2Si_2O_8$ phase. The XRD patterns of x = 0.2–0.6 showed that the ceramics crystallized in a single phase without a hexagonal phase. This result indicated that solid solutions were formed. However, when x = 0.8, a mixture of $BaZnSi_3O_8$ (~80 mol%) main phase and second phases such as $BaSiO_3$ (~18 mol%) and little SiO_2 (~2 mol%) formed, as shown in Fig. 1(d). This result indicated that the maximum solubility of $BaAl_{2-2x}(ZnSi)_xSi_2O_8$ is located between 0.6 and 0.8.

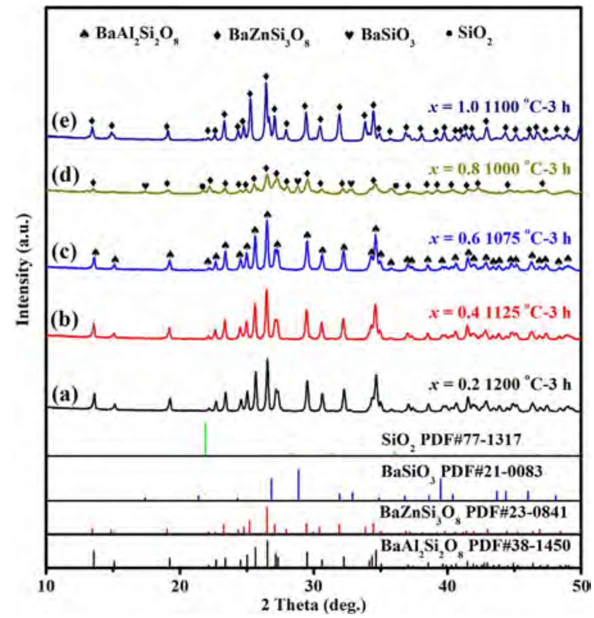

Fig. 1. The XRD patterns of $BaAl_{2-2x}(ZnSi)_xSi_2O_8$ (x = 0.2–1.0) ceramics sintered at different densification temperatures: (a) x = 0.2, 1200 °C; (b) x = 0.4, 1125 °C; (c) x = 0.6, 1075 °C; (d) x = 0.8, 1000 °C; (e) x = 1.0, 1100 °C.

Fig. 2 presents the microstructures and grain size distributions of thermally etched $BaAl_{2-2x}(ZnSi)_xSi_2O_8$ (x = 0.2–1.0) ceramics sintered at different temperatures. Dense and homogeneous microstructures were present in x = 0.2 and x = 0.4. With the substitution of $(Zn_{0.5}Si_{0.5})^{3+}$ for Al^{3+}, the ceramics became more sensitive to sintering temperature. Hence, when x increased to 0.6 and 1.0, some abnormal grain growth and little porosity was observed in Fig. 2(c) and (e). As for x = 0.8, the distribution of grain was disorganized, which was attributed to the effects of multi-phases and glass. The average grain size estimated from insets in Fig. 2(a)–(e) was about 1.02, 1.11, 1.27, 0.95, and 1.04 μm corresponding to x = 0.2, 0.4, 0.6, 0.8, and 1.0. The grain growth was promoted when x increased from 0.2 to 0.6. The distribution of grain size for x = 0.8 and 1.0 was erratic, and the average grain size was slightly reduced.

The bulk densities and the relative densities of $BaAl_{2-2x}(ZnSi)_xSi_2O_8$ (x = 0.2–1.0) ceramics sintered at different temperatures for 3 h are demonstrated in Fig. 3. The bulk densities of $BaAl_{2-2x}(ZnSi)_xSi_2O_8$ (x = 0.2–0.8) initially increased with increasing sintering temperature and decreased after reaching their maximum value. However, the bulk densities of $BaAl_{2-2x}(ZnSi)_xSi_2O_8$ (x = 1.0) linearly increased until a molten trace appeared at sintering temperatures exceeding 1100 °C. Thus, we disregarded the microwave dielectric properties of $BaAl_{2-2x}(ZnSi)_xSi_2O_8$ (x = 1.0) sintered at temperatures above 1100 °C. The maximum densities of the ceramics also increased initially and then decreased above x = 0.8 with increasing x. On one hand, maximum density increased with increasing atomic weight. On the other hand, porosity affected maximum density. Therefore, as the $(Zn_{0.5}Si_{0.5})$ dopant with higher weight than the Al atom, maximum density showed an increasing tendency. Whereas glass phase promoted

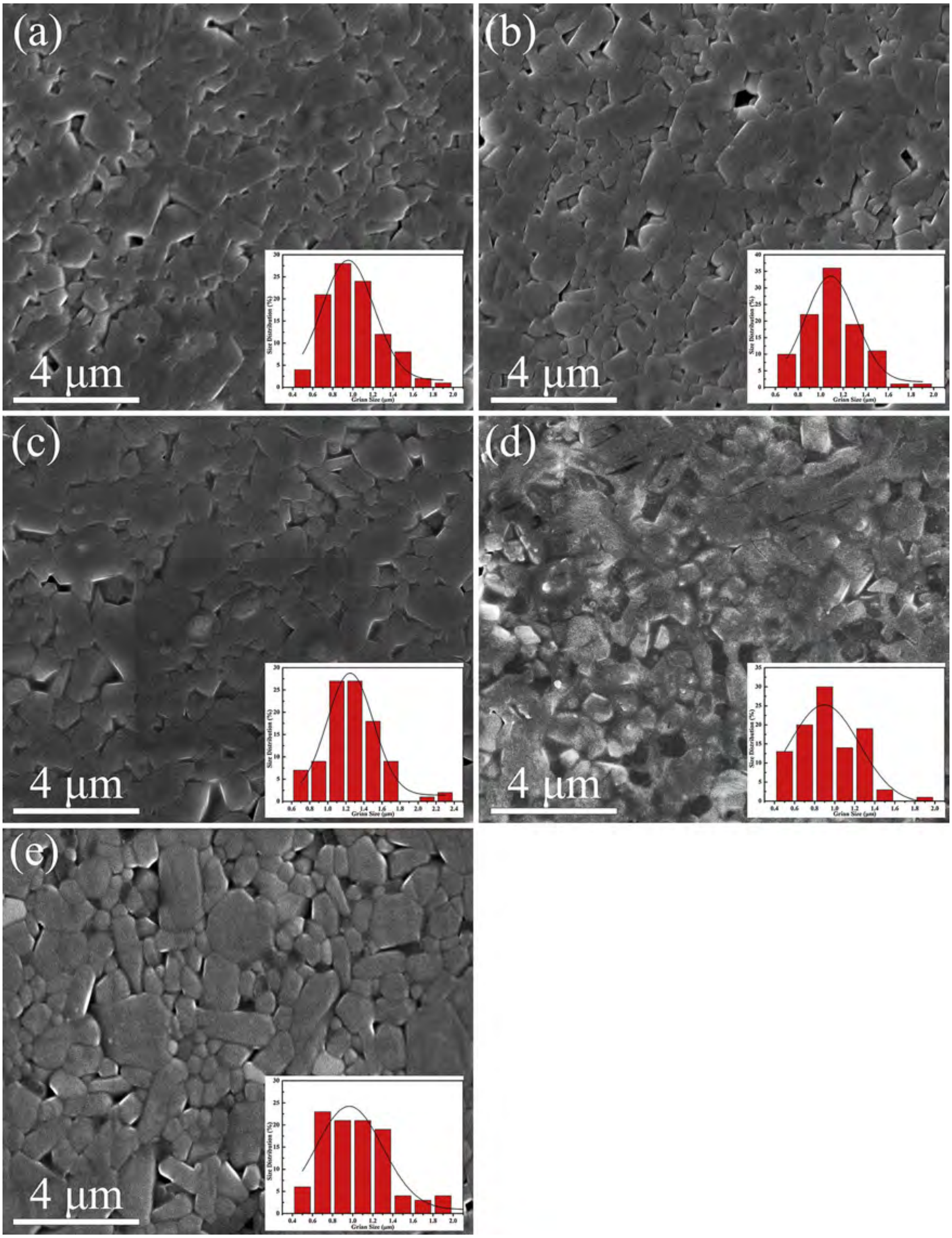

Fig. 2. SEM images and grain size distributions (insets) of thermally etched $BaAl_{2-2x}(ZnSi)_xSi_2O_8$ (x = 0.2–1.0) ceramics sintered at different densification temperatures: (a) x = 0.2, 1200 °C; (b) x = 0.4, 1125 °C; (c) x = 0.6, 1075 °C; (d) x = 0.8, 1000 °C; and (e) x = 1.0, 1100 °C.

the densification of $BaAl_{2-2x}(ZnSi)_xSi_2O_8$ (x = 0.8) (Fig. 2(d)), so it exhibited higher maximum density than $BaAl_{2-2x}(ZnSi)_xSi_2O_8$ (x = 1.0) (Fig. 3(a)). The variation tendency of density for each composition sharpened with increasing x, indicating that the ceramics became more sensitive to sintering temperature. The maximum relative density for each composition was higher than 95%, however, the relative density of $BaZnSi_3O_8$ was smaller than other compositions.

Fig. 4 shows the relative permittivity of $BaAl_{2-2x}(ZnSi)_xSi_2O_8$ (x = 0.2–1.0) ceramics sintered at different temperatures for 3 h. The correlations between ε_r and sintering temperature exhibited the same trend as those between relative density and sintering temperature (Figs. 3 and 4). For different compositions, the maximum ε_r value is controlled by ionic polarizability, porosity, and so on [29]. The ionic polarisability of $(Zn_{0.5}Si_{0.5})^{3+}$ (1.455 Å^3) is larger than that of Al^{3+} (0.79 Å^3) [30]; thus, the ε_r of $BaAl_{2-2x}(ZnSi)_xSi_2O_8$ (x = 0.2–0.6) showed a gradually increasing trend [13]. However, when the x reached 0.8, ε_r dramatically decreased. The decrease in relative permittivity for x = 0.8 should be attributed to the glass phase and low relative permittivity of $BaZnSi_3O_8$. By contrast, the decrease in relative permittivity for x = 1.0 arose from changes in lattice structure and

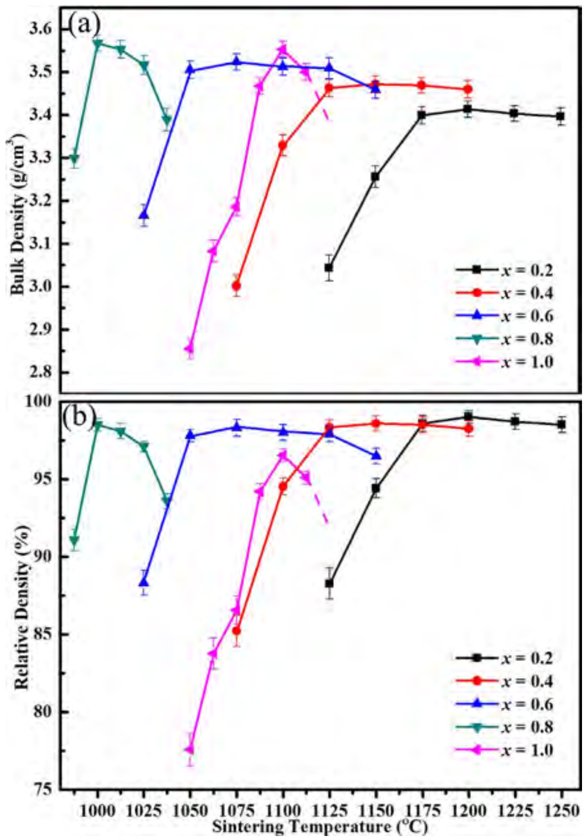

Fig. 3. (a) The bulk density and (b) the relative density of $BaAl_{2-2x}(ZnSi)_xSi_2O_8$ (x = 0.2–1.0) ceramics as a function of sintering temperatures for 3 h.

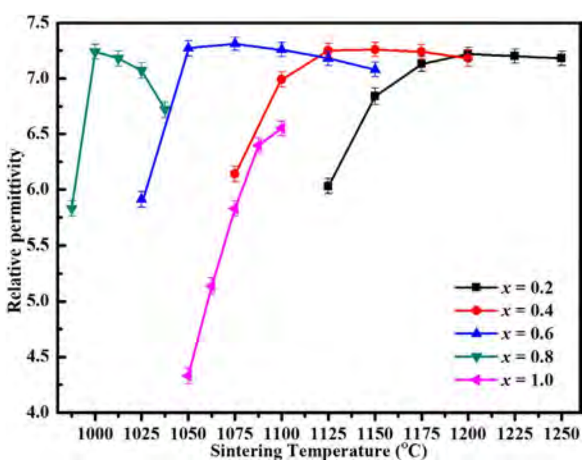

Fig. 4. The relative permittivity (at 15.0–15.5 GHz) of $BaAl_{2-2x}(ZnSi)_xSi_2O_8$ (x = 0.2–1.0) ceramics as a function of sintering temperatures for 3 h.

densification (Fig. 1).

Table 1 shows the theoretical relative permittivity of $BaAl_{2-2x}(ZnSi)_xSi_2O_8$ (x = 0.2–0.6 and 1.0) compounds calculated with the polarisability suggested by Shannon and the Clausius–Mosotti equation [30]. The trend of calculated ε_r versus the composition agreed well with the experimental result except for that of x = 1.0 due to the structural changes and poor density of $BaAl_{2-2x}(ZnSi)_xSi_2O_8$ (x = 1.0) (Fig. 3). The positive deviations (Δ,%) between experimental and theoretical relative permittivity are observed in Table 1. In fact, the Clausius-Mossotti equation is suitable for high symmetric crystal materials with ion displacing polarisation. The distorted polyhedrons occurred in low symmetric crystal structure, which led to the emergence of "rattling" cations in the center of polyhedron with corresponding high polarisabilites [31]. Thus, the deviations (Δ,%) between experimental and theoretical relative permittivity of $BaAl_{2-2x}(ZnSi)_xSi_2O_8$ resulted from its low symmetry (monoclinic). Moreover, the Δ, % value reduced dramatically at 1.0 due to its lowest relative density (Fig. 3(b)).

Table 1
Comparison of the calculated and experimental relative permittivity of some silicate and germanate ceramics.

Composition	x	ε_{calc}	ε_{exp}	Δ,%	Ref.
$BaZnSiO_4$	–	7.71	12.20	+36.80	[1]
$Bi_4Si_3O_{12}$	–	11.8	14.20	+16.90	[30,32]
$K_xBa_{1-x}Ga_{2-x}Ge_{2+x}O_8$	0.6	4.83	6.10	+28.20	[14]
	0.67	4.76	6.0	+20.67	
	0.9	4.58	5.60	+18.21	
	1.0	4.49	5.50	+18.36	
$CaAl_2Si_2O_8$	–	4.70	7.14	+34.17	[30]
$BaAl_{2-2x}(ZnSi)_xSi_2O_8$	0	5.21	7.20	+27.64	[13]
	0.2	5.34	7.22	+26.04	This work
	0.4	5.46	7.25	+24.69	
	0.6	5.58	7.31	+23.67	
	1.0	5.60	6.60	+15.15	

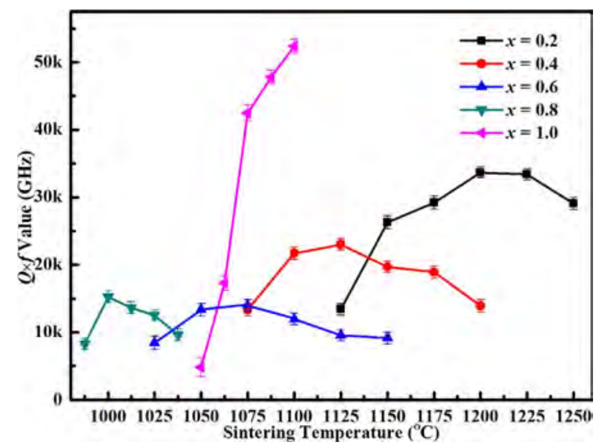

Fig. 5. The $Q \times f$ value (at 15.0–15.5 GHz) of $BaAl_{(2-2x)}(ZnSi)_xSi_2O_8$ (x = 0.2–1.0) ceramics as a function of sintering temperatures for 3 h.

Fig. 5 shows the $Q \times f$ values of $BaAl_{2-2x}(ZnSi)_xSi_2O_8$ (x = 0.2–1.0) solid solutions sintered at different temperatures for 3 h. As sintering temperature increased, the $Q \times f$ of each composition increased to a maximum value before decreasing. The change in maximum $Q \times f$ value exhibited a trend that opposed that of the relative permittivity as x increased from 0.2 to 1.0. A maximum $Q \times f$ value of 52401 GHz was obtained for $BaZnSi_3O_8$ (x = 1.0). The density, second phase and glass phase not only influenced the relative permittivity but also dielectric loss. Compared with $BaAl_2Si_2O_8$ (x = 0), $BaZnSi_3O_8$ (x = 1.0) possessed a similar relative permittivity of approximately 6.60, but a higher $Q \times f$ value and a considerably lower sintering temperature [15].

The τ_f value is related to the coefficient of thermal expansion α_l and the temperature coefficient of relative permittivity τ_ε, and can be calculated as follows [33]:

$$\tau f = -\alpha l - \frac{1}{2}\tau\varepsilon \tag{2}$$

α_l is approximately 10 ppm/°C for oxide ceramics [34]. τ_ε can be calculated with [35]:

$$\tau\varepsilon = \frac{1}{\varepsilon}\left(\frac{\partial\varepsilon}{\partial T}\right)_P = \left(\varepsilon - \frac{2}{\varepsilon} + 1\right)(A + B + C)$$
$$A = \frac{1}{3V}\left(\frac{\partial V}{\partial T}\right)_P,\quad B = \frac{1}{3\alpha_m}\left(\frac{\partial\alpha_m}{\partial V}\right)_T\left(\frac{\partial V}{\partial T}\right)_P,\quad C = \frac{1}{3\alpha_m}\left(\frac{\partial\alpha_m}{\partial T}\right)_P \tag{3}$$

As inferred from Eqs. (2) and (3), τ_f is mainly determined by ε_r and the slope of ε_r-T. When τ_ε is negative, τ_f increases with the relative

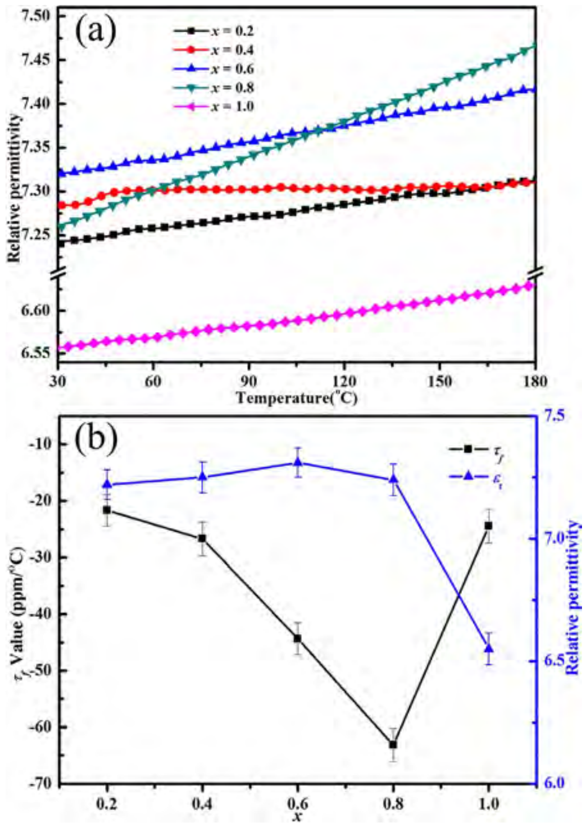

Fig. 6. (a) The dependence of relative permittivity (ε_r) on temperature at 1 MHz (b) τ_f and ε_r value (at 15.0–15.5 GHz) for well sintered $BaAl_{2-2x}(ZnSi)_xSi_2O_8$ (x = 0.2–1.0) ceramics.

permittivity. When τ_ε is positive, τ_f decreases with relative permittivity [36]. Fig. 6(a) shows the temperature dependence of relative permittivity (ε_r) at 1 MHz for $BaAl_{2-2x}(ZnSi)_xSi_2O_8$ (x = 0.2–1.0) ceramics. The relative permittivity of each composition increased with increasing temperature, indicating that τ_ε is positive. The slope of ε_r-T slowly increased as x increased from 0.2 to 0.8 and decreased thereafter. However, the nonlinear phenomenon appeared for x = 0.4, this phenomenon may be caused by phase transition [1,37,38]. Thus, the slope variation of ε_r-T had a similar trend with that of ε_r, and τ_f has an opposite trend with that of ε_r (Fig. 6(b)). It was noted that the τ_f value at microwave frequency of about 15 GHz agreed well with the slope of ε_r-T curve (τ_ε) at 1 MHz based on Eq. (2), which indicated that the measuring frequency above 1 MHz seldom affected on the change tendency of ε_r with T of the $BaAl_{2-2x}(ZnSi)_xSi_2O_8$ ceramics.

4. Conclusions

The sintering behaviour and microwave dielectric properties of $BaAl_{2-2x}(ZnSi)_xSi_2O_8$ (x = 0.2–1.0) solid solutions were investigated in this study. Substituting $(Zn_{0.5}Si_{0.5})$ for Al in $BaAl_2Si_2O_8$ considerably decreased sintering temperature from 1475 °C ($BaAl_2Si_2O_8$) to 1100 °C ($BaZnSi_3O_8$). $BaAl_{2-2x}(ZnSi)_xSi_2O_8$ (x = 0.2–0.6 and 1.0) solid solutions did not exhibit a hexagonal phase and microcracks, and $(Zn_{0.5}Si_{0.5})^{3+}$ substitution significantly improved the phase stability of $BaAl_2Si_2O_8$. The maximum solubility of $BaAl_{2-2x}(ZnSi)_xSi_2O_8$ was between 0.6 and 0.8 for x, and a low temperature eutectic was obtained at x = 0.8. Composition and density strongly dominated the microwave dielectric. The variation in relative permittivity and $Q \times f$ value exhibited the same trend as that of bulk density for each composition. The ε_r value gradually increased and reached a maximum value of 7.31 at x = 0.6 before decreasing. The variation of $Q \times f$ value had an opposite trend with that of ε_r value. The τ_f reached the maximum negative value of −63 ppm/°C at x = 0.8. A new type of plagioclase $BaZnSi_3O_8$ was prepared at 1100 °C, which possesses good microwave dielectric properties with ε_r = 6.60, $Q \times f$ = 52401 GHz (at 15.4 GHz) and τ_f = −24.5 ppm/°C and a medium sintering temperature. However, the sensitive sinterability and slightly negative τ_f value of $BaZnSi_3O_8$ have to be improved in the future.

Acknowledgements

This work was supported by the National Natural Science Foundation of China (NSFC-51572093, 51772107, and 61771215). The authors are grateful to the Analytical and Testing Center, Huazhong University of Science and Technology, for SEM analyses.

References

[1] Z.Y. Zou, Z.H. Chen, X.K. Lan, W.Z. Lu, B. Ullah, X.H. Wang, W. Lei, Weak ferroelectricity and low-permittivity microwave dielectric properties of $Ba_2Zn_{(1+x)}Si_2O_{(7+x)}$ ceramics, J. Eur. Ceram. Soc. 37 (2017) 3065–3071.
[2] S. Wu, C. Jiang, Y. Mei, W. Tu, Synthesis and microwave dielectric properties of Sm_2SiO_5 ceramics, J. Am. Ceram. Soc. 95 (2012) 37–40.
[3] Y. Guo, H. Ohsato, K. Kakimoto, Characterization and dielectric behavior of willemite and TiO_2-doped willemite ceramics at millimeter-wave frequency, J. Eur. Ceram. Soc. 26 (2006) 1827–1830.
[4] K.X. Song, X.M. Chen, C.W. Zheng, Microwave dielectric characteristics of ceramics in Mg_2SiO_4-Zn_2SiO_4 system, Ceram. Int. 34 (2008) 917–920.
[5] J. Zhang, Y. Zhou, B. Peng, Z. Xie, X. Zhang, Z. Yue, Microwave dielectric properties and thermally stimulated depolarization currents of MgF_2-doped diopside ceramics, J. Am. Ceram. Soc. 97 (2014) 3537–3543.
[6] K.N. Lee, D.S. Fox, J.I. Eldridge, D. Zhu, R.C. Robinson, N.P. Bansal, R.A. Miller, Upper temperature limit of environmental barrier coatings based on mullite and BSAS, J. Am. Ceram. Soc. 86 (2003) 1299–1306.
[7] W.B. Im, Y. Kim, D.Y. Jeon, Thermal stability study of $BaAl_2Si_2O_8$: Eu^{2+} phosphor using its polymorphism for plasma display panel application, Chem. Mater. 18 (2006) 1190–1195.
[8] N.P. Bansal, J.A. Setlock, Fabrication of fiber-reinforced celsian matrix composites, Compos. Part A – Appl. Sci. Manuf. 32 (2001) 1021–1029.
[9] R.A. McCauley, Polymorphism and dielectric electric properties of Ba-and Sr-containing feldspars, J. Mater. Sci. 35 (2000) 3939–3942.
[10] M.M. Krzmanc, M. Valant, D. Suvorov, A structural and dielectric characterization of $Na_xCa_{1-x}Al_{2-x}Si_{2+x}O_8$ (x = 0 and 1) ceramics, J. Eur. Ceram. Soc. 25 (2005) 2835–2838.
[11] M.M. Krzmanc, M. Valant, B. Jancar, D. Suvorov, Sub-solidus synthesis and microwave dielectric characterization of plagioclase feldspars, J. Am. Ceram. Soc. 88 (2005) 2472–2479.
[12] M.M. Krzmanc, A. Meden, D. Suvorov, The correlation between the structure and the dielectric properties of $K_xBa_{1-x}Ga_{2-x}Ge_{2+x}O_8$ ceramics, J. Eur. Ceram. Soc. 27 (2007) 2957–2961.
[13] M.M. Krzmanc, M. Valant, D. Suvorov, The synthesis and microwave dielectric properties of $Sr_xBa_{1-x}Al_2Si_2O_8$ and $Ca_yBa_{1-y}Al_2Si_2O_8$ ceramics, J. Eur. Ceram. Soc. 27 (2007) 1181–1185.
[14] N. Qin, M.M. Krzmanc, A. Meden, D. Suvorov, Structural investigation of $K_xBa_{1-x}Ga_{2-x}Ge_{2+x}O_8$ solid solutions using the X-ray Rietveld method, J. Solid State Chem 182 (2009) 1666–1672.
[15] W. Lei, R. Ang, X.C. Wang, W.Z. Lu, Phase evolution and near-zero shrinkage in $BaAl_2Si_2O_8$ low-permittivity microwave dielectric ceramics, Mater. Res. Bull. 50 (2014) 235–239.
[16] K.M. Manu, C. Karthik, R. Ubic, M.T. Sebastian, Effect of Ca^{2+} substitution on the structure microstructure, and microwave dielectric properties of $Sr_2Al_2SiO_7$ ceramic, J. Am. Ceram. Soc. 96 (2013) 3842–3848.
[17] C.W. Zheng, S.Y. Wu, X.M. Chen, K.X. Song, Modification of $MgAl_2O_4$ microwave dielectric ceramics by Zn substitution, J. Am. Ceram. Soc. 90 (2007) 1483–1486.
[18] W. Lei, W.Z. Lu, J.H. Zhu, F. Liang, D. Liu, Modification of $ZnAl_2O_4$-based low-permittivity microwave dielectric ceramics by adding 2MO-TiO_2 (M = Co, Mg, and Mn), J. Am. Ceram. Soc. 91 (2008) 1958–1961.
[19] W. Jin, W. Yin, S. Yu, M. Tang, T. Xu, B. Kang, H. Huang, Microwave dielectric properties of pure YAG transparent ceramics, Mater. Lett. 173 (2016) 47–49.
[20] K.T. Lee, P.B. Aswath, Role of mineralizers on the hexacelsian to celsian transformation in the barium aluminosilicate (BAS) system, Mater. Sci. Eng. A – Struct. 352 (2003) 1–7.
[21] C.B. Sclar, Iron in lunar anorthite: substitutional mechanism and subsolidus history, Meteorit. Planet. Sci. 14 (1979) 531–531.
[22] B. Liu, L. Li, X.Q. Liu, X.M. Chen, Structural evolution of $SrLaAl_{1-x}(Zn_{0.5}Ti_{0.5})_xO_4$ ceramics and effects on their microwave dielectric properties, J. Mater. Chem. C 4 (2016) 4684–4691.
[23] G.R. Ren, J.Y. Zhu, L. Li, B. Liu, X.M. Chen, $SrLa(R_{0.5}Ti_{0.5})O_4$ (R = Mg, Zn) microwave dielectric ceramics with complex K_2NiF_4-type layered perovskite structure, J. Am. Ceram. Soc 100 (2017) 2582–2589.
[24] M. Heuer, K. Bente, M. Steins, Crystal structure of calcium tectozincotrisilicate, $CaZnSi_3O_8$, Z. Kristallogr. NCS 213 (1998) 691–692.
[25] K.T. Fehr, A.L. Huber, Stability and phase relations of $Ca[ZnSi_3]O_8$, a new phase

with feldspar structure in the system CaO-ZnO-SiO_2, Am. Mineral. 86 (2001) 21–28.
[26] E.R. Segnit, A.E. Holland, The ternary system BaO-ZnO-SiO_2, Aust. J. Chem. 23 (1970) 1077–1085.
[27] T. Sugawara, Thermodynamic analysis of Fe and Mg partitioning between plagioclase and silicate liquid, Contrib. Mineral. Petrol. 138 (2000) 101–113.
[28] B.W. Hakki, P.D. Coleman, A dielectric resonant method of measuring inductive capacitance in the millimeter range, IRE Trans. Microwave Theory Tech. 8 (1960) 402–410.
[29] H. Zhou, J. Huang, X. Tan, N. Wang, G. Fan, X. Chen, Compatibility with silver electrode and microwave dielectric properties of low firing $CaWO_4$-$2Li_2WO_4$ ceramics, Mater. Res. Bull. 89 (2017) 150–153.
[30] R.D. Shannon, Dielectric polarizabilities of ions in oxides and fluorides, J. Appl. Phys. 73 (1993) 348–366.
[31] Z.F. Fu, P. Liu, J.L. Ma, X.G. Zhao, H.W. Zhang, Novel series of ultra-low loss microwave dielectric ceramics: Li2Mg3BO6 (B = Ti Sn, Zr), J. Eur. Ceram. Soc. 36 (2016) 625–629.
[32] H. Xie, F. Li, H. Xi, D. Zhou, Microwave dielectric properties of sol-gel processed $Bi_4Si_3O_{12}$ ceramics and single crystal, Trans. Ind. Ceram. Soc. 74 (2015) 83–85.
[33] I.M. Reaney, D. Iddles, Microwave dielectric ceramics for resonators and filters in mobile phone networks, J. Am. Ceram. Soc. 89 (2006) 2063–2072.
[34] K.H. Yoon, E.S. Kim, J.S. Jeon, Understanding the microwave dielectric properties of $(Pb_{0.45}Ca_{0.55})[Fe_{0.5}(Nb_{1-x}Ta_x)_{0.5}]O_3$ ceramics via the bond valence, J. Eur. Ceram. Soc. 23 (2003) 2391–2396.
[35] A.J. Bosman, E.E. Havinga, Temperature dependence of dielectric constants of cubic ionic compounds, Phys. Rev. 129 (1963) 1593–1600.
[36] D. Zhou, C.A. Randall, H. Wang, L.X. Pang, X. Yao, Microwave dielectric properties trends in a solid solution $(Bi_{1-x}Ln_x)_2Mo_2O_9$ (Ln = La Nd, $0.0 \le x \le 0.2$) system, J. Am. Ceram. Soc. 92 (2009) 2931–2936.
[37] T. Nagai, S. Asai, R. Okazaki, I. Terasaki, H. Taniguchi, Effects of element substitution on the pyroelectric phase transition of stuffed-tridymite-type $BaZnGeO_4$, Solid State Commun. 219 (2015) 12–15.
[38] D. Zhou, L.X. Pang, Z.M. Qi, Crystal structure and microwave dielectric behaviors of ultra-Low-temperature fired $x(Ag_{0.5}Bi_{0.5})MoO_4$-$(1-x)BiVO_4$ ($0.0 \le x \le 1.0$) solid solution with scheelite structure, Inorg. Chem. 53 (2014) 9222–9227.